STRESS DISTRIBUTION ON MECHANICALLY SWITCHED CAPACITOR WITH DAMPING NETWORK (MSCDN) REACTOR UNDER SWITCHING CONDITIONS

H. Abdul Hamid*, N.Harid, A. Haddad
High Voltage Energy System Group (HIVES), School of Engineering, Cardiff University, United Kingdom
*Email: abdulhamidH1@cardiff.ac.uk

Abstract: This paper presents an analysis of voltage stresses on the reactor of the MSCDN when subjected to switching surges during its routine energization. Transient voltages of high magnitude and frequency can occur at the reactor of the MSCDN after the closing of the circuit breaker at an unfavourable point-on-wave instant. Under fast transients, the stray inductances and capacitances of the reactor winding will influence the transient voltage distribution along the reactor column. In this paper, a lumped parameter equivalent circuit is developed to assess the distribution of switching surge voltages along the reactor winding. The analytical derivations of the lumped parameter circuit components used for the equivalent circuit are presented. The results indicate that high-frequency oscillatory overvoltages were generated in all sections of reactor winding. The highest voltage magnitudes with rapid rate of change were observed in particular across the top sections of the winding. These voltage stresses may exceed the impulse withstand level of the reactor insulation.

1 INTRODUCTION

The need for air-core reactors has been first highlighted when some electric power applications required that reactors have linear or quasi-linear current/voltage characteristics. Air-cored reactors are preferred in high voltage systems because of their relative low cost and saturation properties, and are used for a variety of applications. The MSCDN filter reactor is one of the most commonly encountered in high voltage substations. Figure 1 shows a one-line diagram of the MSCDN circuit, which is also referred to as C-type filter. In filter applications, air-cored reactors may be exposed to fast rates of rise of voltage as well as switching overvoltages of long duration during filter energization. Localised failure of the turn-to-turn insulation due to non-linear voltage distribution may result under certain conditions. For these reasons, the accurate assessment of the voltage distribution in air-cored reactor windings during transients is vital for reliable operation of the inductor under service conditions.

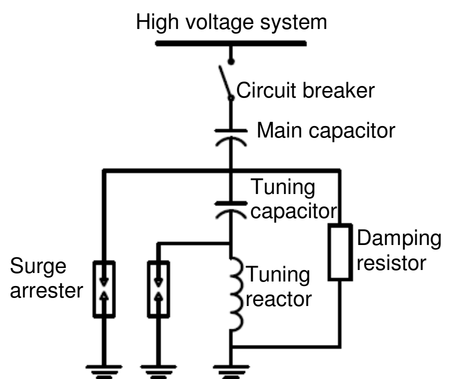

Figure 1: One-line diagram of the MSCDN

The impulse voltage distribution of helical windings has been investigated by many researchers since 1950's [1-6]. Some of these studies focussed mainly on transformer windings when excited by impulse or lightning surges [2, 6]. Fortunately, the methods that were proposed for calculating voltage distribution in transformer windings are also applicable when addressing similar issues in air-cored reactors owing to the similarity in the winding construction.

A number of researchers published methods for computing the voltage distribution in air-cored reactors [1, 5]. In these methods, the reactor winding is usually represented by a ladder network having a finite number of uniform sections. To perform transient analysis on such networks, the winding parameters, including stray capacitances and inductances need to be estimated. Despite similarities in the analysis, different approaches in calculating the winding parameters were adopted in [1] and [5]. In the work described in [5], the reactor winding was represented as a capacitive equivalent circuit. The mutual inductances between turns were not represented, and no resistance was included. The inter-turn capacitances were derived using a parallel-plate capacitance formula. The capacitances to ground were calculated using a formula for a vertical cylinder as proposed in [7]. The work presented in [1] considered almost all relatively important winding parameters for representation of the reactor winding. The mutual inductances, the mutual capacitances, the winding and the dielectric resistances of the winding were all considered in the circuit model. Under impulse conditions, it was suggested that the shunt resistance representing the inter-turn dielectric losses is more important than the series resistance.

In this work, an equivalent circuit of the same general form suggested in [1] is used but the winding parameters of vertically mounted reactor are obtained using significantly different but simple formulae.

2 AIR-CORE REACTOR EQUIVALENT CIRCUIT

To account for the relatively large size of the coil in the following analysis, it is assumed that the reactor winding is physically subdivided into 'k' sections of equal length and radius. Figure 2 illustrates the reactor winding and the physical location of the sections above ground. Assuming that all sections are of sufficiently short length; it is possible to use a lumped parameter approach to represent and analyse the winding response.

Based on the configuration shown in Figure 2, an equivalent circuit representing the reactor winding is developed as shown in Figure 3. Each section consists of the winding-turns inductance L_s, the inter-turn shunt capacitance C_s, the stray capacitance to ground C_g, the winding series resistance R_w and the inter-turn insulation shunt resistance R_d.

3 CALCULATION OF REACTOR WINDING PARAMETERS

3.1 Calculation of inductances

Calculation of self and mutual inductances was carried out using well established formulae as given in [3]. For the self inductance, the formula applicable to single-layer coils on cylindrical winding forms was used, and was applied for all sections given their similarity in construction. Equation (1) allows estimation of the section self inductance:

$$L_k = \frac{0.002\pi^2 a^2 N_k^2 K}{b_k/2a} \qquad (1)$$

where:
L_k= self-inductance of section k (mH)
a= mean radius (cm)
N_k= no. of turns of section k
K= Nagaoka's constant [3]
b_k= length of section k (cm)

The mutual inductance of coaxial single-layer coils was used to obtain the mutual inductances between adjacent and non-adjacent sections of the reactor winding. This formula is applicable for mutual inductance calculation of two coaxial coils having equal radii and length. Equation (2) gives the section mutual inductance:

$$M_{k,k-1} = 0.002\ \pi^2 a^2 n_k^2 [r_1B_1 - r_2B2 - r_3B_3 + r_4B_4] \qquad (2)$$

where:
$M_{k,k-1}$= mutual inductance between section k and section k-1 (mH)
a= mean radius (cm)
n_k= winding density (turns/cm)
r_n= diagonal distances between sections (cm)
B_n= functions B [3]

Finally, the total inductance L_s, as shown in the circuit of Figure 3, is obtained as the sum of the self-inductance of the section and the contributions of mutual inductances due to all the other sections.

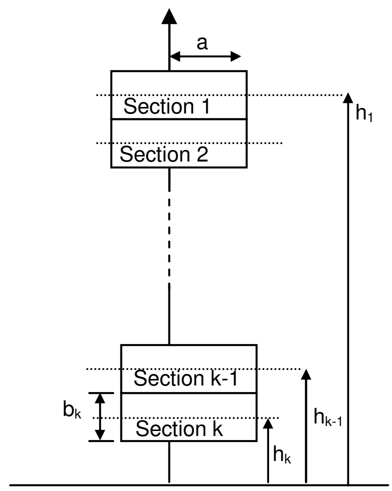

Figure 2: Winding sections (a is the radius of the reactor; b_k is length of section k; h_k is the distance from the ground to the centre of section k.)

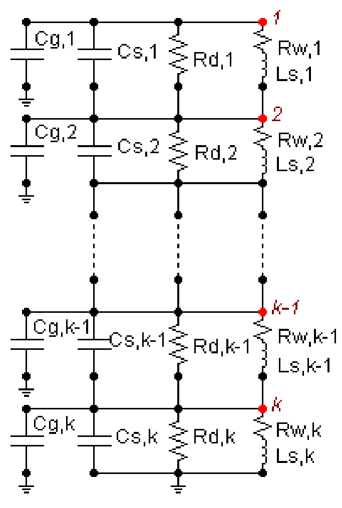

Figure 3: An equivalent circuit of reactor winding

3.2 Calculation of capacitances

The inter-turn shunt capacitance, C_s, and the capacitance to ground, C_g, are calculated based on the parallel-plate capacitance principle. The total inter-turn shunt capacitance of one section was obtained by taking the equivalent of a series connected turn-to-turn capacitances of that section. Equation (3) gives the shunt capacitance of section k:

$$C_{sk} = \frac{(\varepsilon_o \varepsilon_m A_s)/d}{N_k - 1} \tag{3}$$

where:
C_{sk} = inter-turn capacitance section k (F)
ε_o= permittivity of vacuum (F/m)
ε_m= relative permittivity of Mylar
A_s = effective area (m^2)
d = distance between adjacent turns (m)
N_k=number of turns of section k

The effective area A_s is taken as the surface area of half of the conductor surface facing the other winding conductor surface over the turn length of the winding conductor. The distance, d corresponds to twice the thickness of the Mylar polyester film wrapping the conductors.

In the published work [1, 2], the capacitances to ground were computed mostly for reactors in the horizontal layout. The calculation of capacitance to ground for such a configuration is rather simple due to the fact that all sections of reactor winding are located at the same level above ground, and is not applicable for a vertically erected reactor.

By referring to Figure 2, each section is placed at a different height from the ground hence the winding capacitance to ground varies along its length. To calculate this capacitance, Equation (4) is used:

$$C_{gk} = (\varepsilon_o \varepsilon_a A_g)/h_k \tag{4}$$

where:
C_{gk} = capacitance to ground of section k (F)
ε_a= relative permittivity of air
A_g= effective area (m^2)
h_k = distance from the centre of section k to the ground (m)

The effective area A_g can be calculated as the product of the section circumference and height. The section circumference is equal to the perimeter of the cylinder with radius a, and the value is identical for all sections. The height is equal to the sum of half of the length of section k, b_k, and the height of the section above ground. As expected, the calculated value of capacitance is larger for sections closer to the ground, and is decreasing with increasing height.

Extensive formulae for calculating the capacitance to ground of various practical configurations can be found in reference [7]. Table 1 shows the capacitance to ground calculated using the proposed Equation (4) and the expression given in [7].

Table 1: Computation of capacitance to ground based on two different formulas

Capacitance	Eqn.(2) pF	Ref. [7] pF	Difference (%)
Cg1	2.516	2.426	3.6
Cg2	2.796	2.683	4.0
Cg3	3.146	3.000	4.6
Cg4	3.597	3.403	5.4
Cg5	4.199	3.931	6.4
Cg6	5.042	4.653	7.7
Cg7	6.309	5.701	9.6
Cg8	8.427	7.363	12.6
Cg9	12.684	10.413	17.9
Cg10	25.637	17.964	29.9

3.3 Series and shunt resistance calculations

The series resistance, R_w of the circuit represents the total current dependent losses. It is assumed that these losses are mainly determined by the winding conductor resistance [1]. Equation (5) gives the series resistance of section k, R_{wk} for the winding length of section k:

$$R_{wk} = (\rho \ell_w)/A_w \tag{5}$$

where:
R_{wk} = winding resistance of section k (Ω)
ρ = conductor resistivity (Ωm)
l_w = total winding length of section k (m)
A_w = cross-sectional area (m^2)

The shunt resistance, R_d representing the inter-turn insulation losses is calculated based on the parallel equivalent circuit model of dielectric losses [1]. This formula is given in terms of the dissipation factor of the dielectric material. Assuming the dielectric losses to be dominant at a certain frequency, the resistance is calculated using the dissipation factor at that frequency as shown in Equation (6)

$$R_{dk} = 1/(2\pi f_d C_{sk} D) \tag{6}$$

where:
R_{dk} = shunt resistance of section k (Ω)
f_d = dominant frequency (Hz)
C_{sk} = shunt capacitance of section k (F)
D = dissipation factor

4 COMPUTATION OF SWITCHING SURGE RESPONSES

With the reactor winding parameters calculated in section 3, computations of transient voltages and currents were performed using the ATP program. Figure 4 shows the full simulation circuit comprising of all elements of the MSCDN. The transient voltages and currents were previously computed with the tuning reactor modelled as a single lumped inductor and the results were published in previous paper [4]. In this paper, the detailed reactor model was added to investigate the voltage distribution along its length. For computation purposes, the reactor length was subdivided into 10 sections having equal axial length along the reactor column.

4.1 Node-to-Ground Voltages

To investigate the surge voltage distribution, the circuit breaker was specified to close at the instant of voltage maximum. In practice, surge arresters are placed across the reactor and across the damping resistor of the MSCDN to improve overvoltage protection.

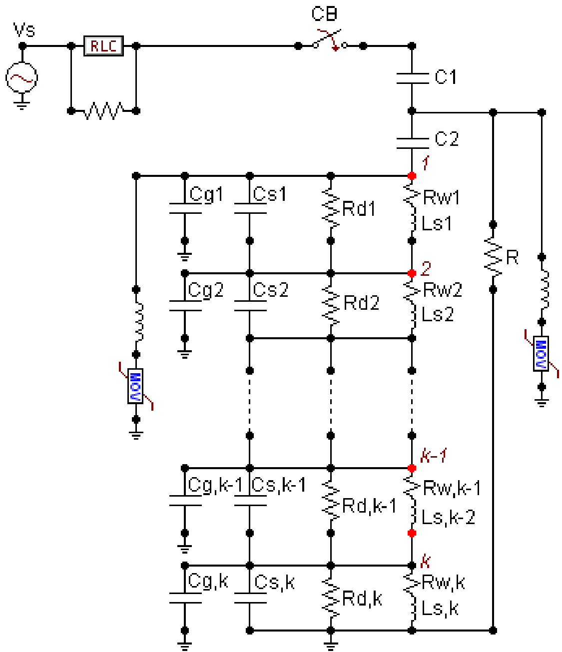

Figure 4: ATP/EMTP Simulation circuit for the MSCDN.

In the simulation, the voltage to ground was recorded at each section of the circuit and the results are presented in Figure 5. The voltage waveform V_1 represents the voltage to ground generated at the reactor terminal after filter energization, which afterwards propagates down the remaining reactor winding. The recorded voltage magnitude of V_1 reaches approximately 225 kV. This value is significantly higher than its actual steady state voltage which is approximately 50 kV. Waveform V_2 gives the voltage to ground measured at 10% of the winding length. Similarly, V_3 to V_5 represent the node voltages occurring at 30% to 50% of the reactor winding.

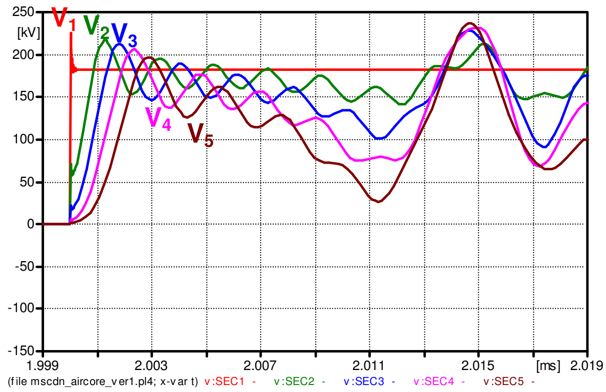

Figure 5: Node voltage to ground (V_1 to V_5 indicate the computed voltages at the 0, 10%, 30%, 40%, 50% along the winding away from the top HV terminal.)

The voltage to ground distribution throughout the winding at various times following the closing of the circuit breaker is presented in Figure 6. At the beginning of the impulse, the highest stresses were observed at the top of the winding. As the impulse propagates along the winding, the stress was redistributed towards the middle of the coil and away from the top.

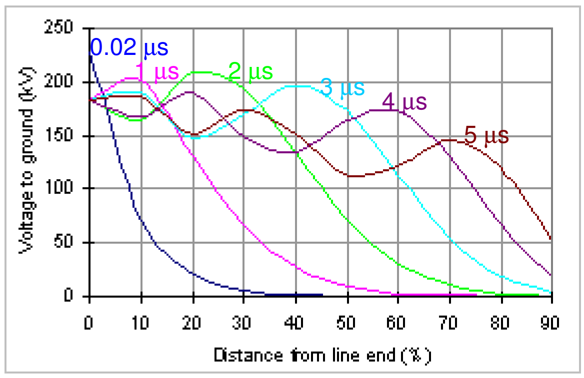

Figure 6: Distribution of node to ground voltages after different times following energisation of the MSDN.

4.2 Node-to-Node Voltages

In addition to the voltage to ground, it is also very important to evaluate the voltages that appear within and across the sections of the reactor winding. Such voltages give information about the stresses imposed on the inter-turn insulation. It must be noted that the stresses in the winding are not only dependent on the voltage amplitude, but also on the rate of voltage change. Figure 7 shows the voltages developed across top 10%, 20% and 50% sections of the winding length starting from the top high voltage terminal of the reactor; these are labelled as V_{s1}, V_{s2}, and V_{s4} respectively. As can be seen, the magnitude of V_{s1} was above 150 kV. Most importantly, this voltage was generated across a fraction of winding that stretches out to only about one-tenth of the total length. This rapid change in voltage within a small region implies a strong electric field, and high stress on the turn-to-turn insulation.

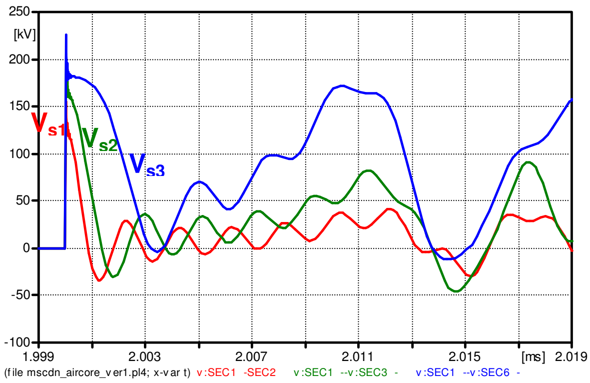

Figure 7: Section voltages (V_{s1}, V_{s2} and V_{s3} correspond respectively to first 10%, 20% and 50% of winding starting from the top.)

Further analysis on the section voltages is presented in Figure 8. In this computation, the maximum values of the voltages across sections are calculated, numbered from 1 to 10. For example, the voltage across section 1 represents the voltage difference between section 1 and section 2 voltages. As can be seen, the maximum voltage magnitude is found to appear across the first section at the top of reactor winding.

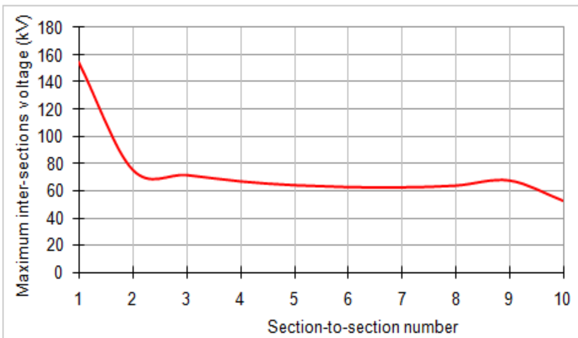

Figure 8: Distribution of maximum voltages along the sections (length of reactor).

4.3 Capacitive and Inductive currents

Following the MSCDN energization, the current that flows through the inter-turn shunt capacitance, C_s is shown to exhibit a more pronounced effect than the currents of the series R_w-L_s branch. The response of capacitive and inductive currents of the circuit is shown in Figure 9. For a better comparison, the capacitive current (I_C) scale is shown on the secondary y-axis.

During the first few microseconds following the switching operation, the magnitude of the capacitive current reaches nearly 50 A, in which time the inductive current of the circuit was comparatively negligible. The voltages shown previously in Figure 7 can be associated with the response obtained here, since the currents flowing across the capacitances are closely dependent on the voltage gradient. The main outcome of this high initial inter-turn capacitive current is the degradation it can cause to the insulation leading to weak points in the insulation. These may then be further damaged through thermal effects on application of main voltage during in-service duties. Such finding may explain some of the intriguing failures experienced in the field.

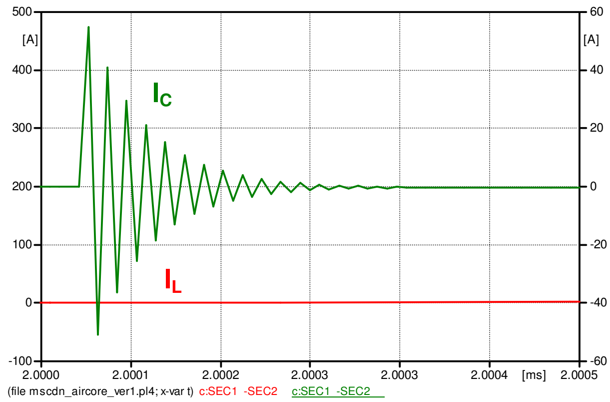

Figure 9: Capacitive (I_C) and inductive (I_L) currents

5 CONCLUSION

The computation of voltage distribution along the MSCDN reactor winding was presented. A detailed model of the air-core reactor based on a lumped parameter equivalent circuit was derived taking into consideration all important winding constants that may affect the transient performance of the reactor. The circuit was simulated successfully in ATP/EMTP program to determine the voltage and current responses during energization of the MSCDN. The results indicated the occurrence of high-frequency transient overvoltages at all sections of the reactor winding.

High voltage magnitude and rapid rate of voltage changes were observed in particular across the top sections of reactor winding. During voltage application, these sections which are located at top high voltage terminal of the reactor winding are severely stressed. The stress may exceed the withstand impulse level used for the design and/or performance of the reactor. Therefore, even transient voltages with peak values below the surge arrester protection level may lead to damage of the reactor.

6 REFERENCES

[1] A.A. Dahab, P.E. Burke and T.H.Fawzi, "A Complete Model of a Single Layer Air-Cored Reactor for Impulse Voltage Distribution', IEEE Trans. Power Delivery, Vol.3, No.4, pp.1745-1753, 1988.

[2] B.M.Dent, E.R.Hartill, J.E.Miles, "A Method of Analysis of Transformer Impulse Voltage Distribution Using a Digital Computer", Proc. IEE, Vol.105, Pt.A.,pp.445-459, 1958.

[3] F.Grover, *Inductance Calculations; Working Formulas and Tables*. New York: Van Nostrand, 1946.

[4] H.Abdul Hamid, N.Harid, and A.Haddad, "Transient Analysis during Switching of Mechanically Switched Capacitor and Damping Network", the 45th International Universities Power Engineering Conference (UPEC), Cardiff, UK, pp.1-4, 2010.

[5] M.M.A. Salama, "A Calculation Method for Voltage Distribution in a Large Air Core Power Reactor", IEEE Trans. PAS, Vol. PAS-100, No.4, pp.1752-1758, 1981.

[6] R. Kasturi and G.R.K. Murthy, "Computation of Impulse Voltage Stresses in Transformer Windings", Proc. IEEE, Vol.126, No.5, 1979.

[7] P. Sarma Maruvada and N. Hylten-Cavallus, "Capacitance Calculations for Some Basic High Voltage Electrode Configurations", IEEE Trans. PAS, Vol.PAS-94, pp.1708-1713, 1975.